



The impact of Gaia on microlensing: the cases of Gaia20bof and Gaia21blx

Paolo Rota*, E. Bachelet, V. Bozza, Y. Tsapras, M. Hundertmark, J. Wambsganss, Ł. Wyrzykowski, R.A. Street,

R. Figuera Jaimes, A. Cassan, M. Dominik, S. Awipan, S. Zola, K. A. Rybicki, M. Jabłonska, P. Mikołajczyk, P. Zielinski, M. Gromadzki, M. Ratajczak, M. Sitek and MiNDSTeP consortium

26th International Microlensing Conference *Livermore 31 January—02 February*

Abstract

With the new generation of large-sky surveys we can detect microlensing events across the entire sky. For this purpose the Gaia satellite becomes fundamental. Thanks to its periodical observations that cover our galaxy, more than 350 microlensing events have been detected and more than 1700 predicted. In this work two microlensing events are shown. High cadence follow-up observations were obtained by the OMEGA Project for both events. The first is Gaia20bof, a binary lens system with degenerate models with spectroscopic observations that indicate that the source is located at <2.2 kpc. The second is Gaia21blx, a binary lens system located in the disk where source and blend, that is attributed to the lens, have comparable magnitude. Using the Gaia parallax and considering it as the flux weighted average parallax of lens and source we can get information about the lens system. In addition to this assumption we consider also information obtained from finite source effects and microlensing obtaining a binary system composed by a G star and K star at 2.2 kpc, while the source is a subgiant F star located at 2.4 kpc. These investigations demonstrate the power of microlensing in detecting low-mass binary systems throughout the Galaxy.

Introduction

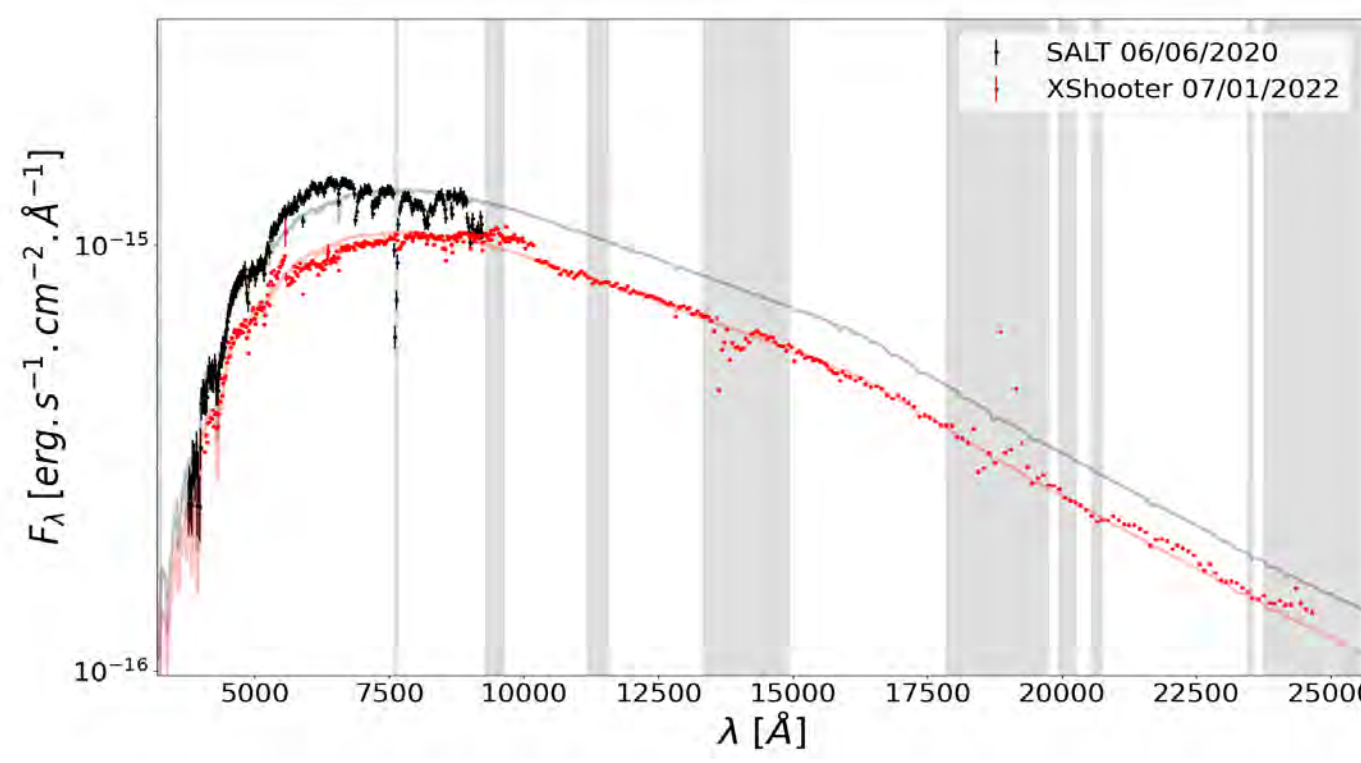
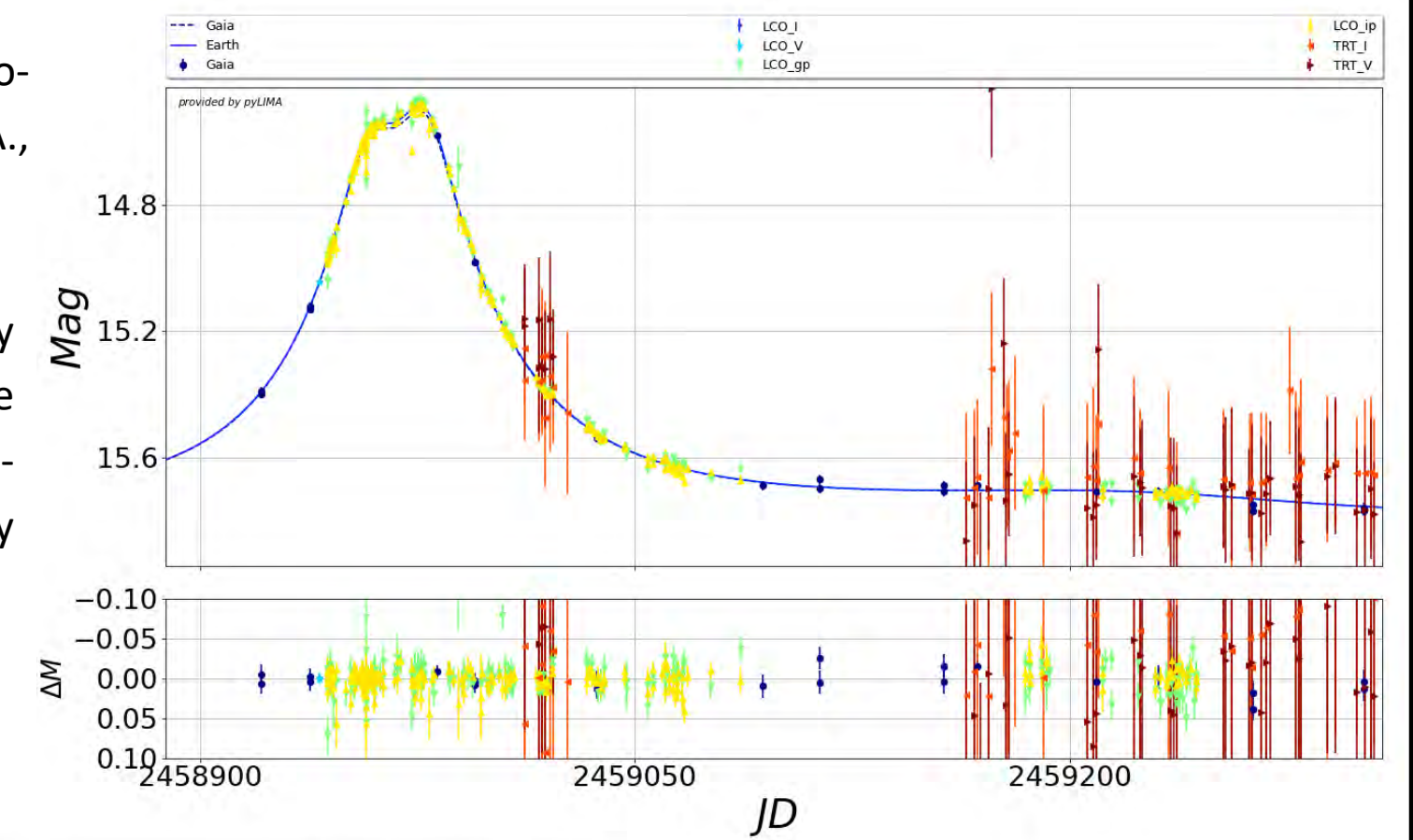
The gravitational microlensing effect has been used for more than twenty years to detect faint objects in the Milky Way. With this technique more than 150 exoplanets have been discovered. In recent years, microlensing has become a unique tool for the identification of planets around faint objects, planets that otherwise could not be detected with other techniques. In particular, with gravitational microlensing we can study binary systems irrespective of the luminosity of their components, since it is the result of their gravitational influence on the light of a background source that is detected, not their intrinsic luminosity; in this way we are able to find exoplanets orbiting single or binary stars brown dwarfs or compact objects like black holes or stellar remnants. With the new generation of large-sky surveys we are able to find microlensing events in the entire sky. And for this purpose the work of Gaia is of fundamental importance given its mission to build an extremely detailed three-dimensional map of the Milky Way. Events observed by Gaia are often of special interest for several reasons. The duration of events in the Galactic Disk is usually longer, allowing the detection of additional effects such as the microlensing parallax or the orbital motion of the lens. In this work we present two events alerted by the Gaia Science Alerts. The first is Gaia20bof, a close binary lens system where also the planetary solutions is considered and Gaia21blx, another binary lens system located in the Galactic Disk. For the former an interesting method to find the physical properties is introduced, where the parallax measured by Gaia is of extreme importance.

Gaia20bof [1]

Parameters	Unit	CloseB-	CloseB+	CloseP-	CloseP+	Resonant-	Resonant+	Wide-	Wide+
t_0	JD	2458971.83 ^{+0.16} _{-0.17}	2458971.90 ^{+0.23} _{-0.17}	2458969.458 ^{+0.074} _{-0.075}	2458969.360 ^{+0.088} _{-0.098}	2458969.427 ^{+0.066} _{-0.063}	2458969.342 ^{+0.080} _{-0.085}	2458927.7 ^{+0.033} _{-0.039}	2458847.2 ^{+0.027} _{-0.024}
u_0		-0.2744 ^{+0.0093} _{-0.0093}	0.2552 ^{+0.0065} _{-0.0073}	-0.29 ^{+0.01} _{-0.03}	0.225 ^{+0.012} _{-0.02}	-0.306 ^{+0.012} _{-0.015}	0.254 ^{+0.012} _{-0.012}	-0.12 ^{+0.012} _{-0.02}	1.66 ^{+0.11} _{-0.10}
b_0	days	56.6 ^{+1.2} _{-1.2}	63.9 ^{+1.5} _{-1.5}	55.0 ^{+3.0} _{-3.0}	67.9 ^{+1.5} _{-1.5}	53.9 ^{+1.9} _{-1.9}	69.9 ^{+1.2} _{-1.2}	49.2 ^{+1.4} _{-1.4}	133.8 ^{+3.7} _{-3.8}
ρ		0.038 ^{+0.013} _{-0.016}	0.017 ^{+0.028} _{-0.018}	0.15 ^{+0.02} _{-0.08}	0.055 ^{+0.019} _{-0.028}	0.1808 ^{+0.0092} _{-0.0096}	0.064 ^{+0.019} _{-0.014}	0.015 ^{+0.013} _{-0.014}	0.037 ^{+0.014} _{-0.019}
s		0.4178 ^{+0.0095} _{-0.0099}	0.4327 ^{+0.0065} _{-0.0064}	0.661 ^{+0.047} _{-0.048}	0.586 ^{+0.017} _{-0.018}	1.013 ^{+0.029} _{-0.023}	1.424 ^{+0.013} _{-0.013}	3.604 ^{+0.043} _{-0.044}	4.082 ^{+0.055} _{-0.056}
q		1.05 ^{+0.11} _{-0.10}	0.84 ^{+0.07} _{-0.07}	0.025 ^{+0.013} _{-0.013}	0.0374 ^{+0.029} _{-0.029}	0.0181 ^{+0.0025} _{-0.0025}	0.0475 ^{+0.0035} _{-0.0035}	0.770 ^{+0.013} _{-0.013}	1.40 ^{+0.12} _{-0.12}
α	rad	0.911 ^{+0.018} _{-0.020}	5.363 ^{+0.019} _{-0.020}	1.643 ^{+0.005} _{-0.005}	4.6527 ^{+0.009} _{-0.009}	1.6452 ^{+0.004} _{-0.004}	4.6517 ^{+0.004} _{-0.004}	0.309 ^{+0.011} _{-0.011}	5.155 ^{+0.021} _{-0.022}
π_{BL}		0.368 ^{+0.015} _{-0.016}	0.227 ^{+0.017} _{-0.019}	0.333 ^{+0.022} _{-0.024}	0.25 ^{+0.01} _{-0.01}	0.341 ^{+0.017} _{-0.013}	0.243 ^{+0.011} _{-0.011}	0.059 ^{+0.025} _{-0.040}	0.082 ^{+0.011} _{-0.008}
π_{BL}		-0.346 ^{+0.014} _{-0.013}	-0.353 ^{+0.014} _{-0.012}	-0.40 ^{+0.02} _{-0.02}	-0.320 ^{+0.014} _{-0.013}	-0.408 ^{+0.023} _{-0.020}	-0.311 ^{+0.013} _{-0.014}	-0.2894 ^{+0.008} _{-0.008}	-0.306 ^{+0.011} _{-0.011}
\mathcal{L}		-6048	-6050	-6052	-6056	-6048	-6057	-6062	-6044
χ^2/dof		720/692	726/692	707/692	721/692	709/692	707/692	723/692	703/692
G_S		15.905 ^{+0.003} _{-0.003}	16.005 ^{+0.003} _{-0.003}	15.87 ^{+0.11} _{-0.11}	16.152 ^{+0.007} _{-0.007}	15.821 ^{+0.074} _{-0.075}	16.156 ^{+0.001} _{-0.001}	16.095 ^{+0.076} _{-0.076}	16.032 ^{+0.004} _{-0.004}
G_B		18.18 ^{+0.31} _{-0.31}	17.60 ^{+0.17} _{-0.17}	18.1 ^{+1.5} _{-1.5}	17.1 ^{+0.2} _{-0.2}	18.8 ^{+1.1} _{-1.1}	17.1 ^{+0.2} _{-0.2}	17.29 ^{+0.19} _{-0.19}	17.44 ^{+0.17} _{-0.17}
G_C		17.055 ^{+0.007} _{-0.008}	17.129 ^{+0.009} _{-0.009}	17.02 ^{+0.11} _{-0.11}	17.265 ^{+0.006} _{-0.006}	16.960 ^{+0.071} _{-0.071}	17.267 ^{+0.006} _{-0.006}	17.237 ^{+0.006} _{-0.006}	17.209 ^{+0.003} _{-0.003}
G_D		19.22 ^{+0.48} _{-0.48}	18.80 ^{+0.18} _{-0.18}	19.3 ^{+1.2} _{-1.2}	18.4 ^{+0.2} _{-0.2}	20.0 ^{+1.1} _{-1.1}	18.4 ^{+0.2} _{-0.2}	18.36 ^{+0.14} _{-0.14}	18.51 ^{+0.15} _{-0.15}
i_S		15.435 ^{+0.007} _{-0.008}	15.510 ^{+0.009} _{-0.009}	15.40 ^{+0.11} _{-0.11}	15.645 ^{+0.006} _{-0.006}	15.340 ^{+0.072} _{-0.072}	15.648 ^{+0.006} _{-0.006}	15.616 ^{+0.006} _{-0.006}	15.589 ^{+0.003} _{-0.003}
i_B		17.25 ^{+0.14} _{-0.14}	16.93 ^{+0.14} _{-0.14}	17.41 ^{+0.95} _{-0.95}	16.56 ^{+0.16} _{-0.16}	17.89 ^{+0.51} _{-0.51}	16.56 ^{+0.17} _{-0.17}	16.58 ^{+0.12} _{-0.12}	16.70 ^{+0.12} _{-0.12}
θ_c	mas	5.5 ± 0.2	5.3 ± 0.2	5.1 ± 0.2	5.4 ± 0.2	5.1 ± 0.2	5.0 ± 0.2	5.5 ± 0.2	5.0 ± 0.2

Gaia20bof is a microlensing event located in the Galactic Disk at (R.A., decl.) = (184.62°, -63.50°).

Most of the data were collected by the Omega Key Project. Using the RTModel platform we get eight degenerate solutions where the binary one is favoured.



Spectra obtained with SALT and XShooter

Microlensing parameters + PARSEC



Old subgiant source, located at 2 kpc.
Binary lens system with a distance > 0.4 kpc and a mass < 0.8 M_sun.

Gaia21blx [2]

Gaia21blx is located in the Galactic Disk at (R.A., decl.) = (14h53m15s.42, -62°01'30".61).

High cadence follow-up observations were obtained by the OMEGA Key Project and also from the MiNDSTeP consortium. Using RTModel platform we get four degenerate solutions. We include orbital motion only for its impact on the error bars of the parallax components. The physical consequences of orbital motion are not considered, as the parameters are not robustly determined. The high blend in all models is attributed solely to the binary lens. From this we assume that the parallax measured by Gaia from the Gaia-DR3 release is the flux-weighted average of lens and source parallaxes. This leads to three constraints, establishing a relationship between lens mass and distance.

C: Close W: Wide +: u0>0 -: u0<0

Parameters	(Unit)	C+	C-	W+	W-
t_0	days	148.3 ^{+8.7} _{-7.0}	134.1 ^{+18.9} _{-18.1}	103.0 ^{+6.8} _{-7.5}	116.7 ^{+10.3} _{-18.7}
u_0	HJD-2450000	9300.29 ^{+0.20} _{-0.31}	9299.66 ^{+0.16} _{-0.34}	9297.38 ^{+0.07} _{-0.08}	9297.96 ^{+0.08} _{-0.08}
ρ_*	10 ⁻³	0.0888 ^{+0.0017} _{-0.00064}	-0.1032 ^{+0.0127} _{-0.0072}	0.0323 ^{+0.0030} _{-0.0030}	-0.0070 ^{+0.0027} _{-0.0006}
α		1.86 ^{+0.15} _{-0.14}	2.13 ^{+0.24} _{-0.30}	2.67 ^{+0.23} _{-0.21}	2.41 ^{+0.21} _{-0.36}
s		-4.875 ^{+0.022} _{-0.018}	4.830 ^{+0.007} _{-0.031}	4.970 ^{+0.014} _{-0.003}	-5.030 ^{+0.080} _{-0.050}
q		0.432 ^{+0.006} _{-0.014}	0.464 ^{+0.017} _{-0.020}	2.013 ^{+0.010} _{-0.001}	1.989 ^{+0.027} _{-0.027}
π_{BL}		0.555 ^{+0.007} _{-0.008}	0.491 ^{+0.023} _{-0.078}	0.233 ^{+0.013} _{-0.009}	0.210 ^{+0.017} _{-0.016}
π_{EL}		0.134 ^{+0.018} _{-0.013}	0.088 ^{+0.056} _{-0.007}	0.233 ^{+0.022} _{-0.059}	0.185 ^{+0.028} _{-0.062}
π_{EL}		0.018 ^{+0.014} _{-0.035}	-0.073 ^{+0.034} _{-0.038}	-0.202 ^{+0.024} _{-0.031}	-0.118 ^{+0.015} _{-0.065}
γ_1	year ⁻¹	-1.32 ^{+0.47} _{-0.29}	-1.76 ^{+0.66} _{-0.44}	0.10 ^{+0.33} _{-0.07}	0.12 ^{+0.47} _{-0.12}
γ_2	year ⁻¹	-0.16 ^{+0.29} _{-0.33}	1.77 ^{+0.58} _{-0.31}	-0.15 ^{+0.22} _{-0.07}	1.34 ^{+0.66} _{-1.02}
γ_3	year ⁻¹	< 1.92	< 2.53	< 1.11	< 2.65
χ^2		477.0	477.9	482.5	485.7
G_S	mag	19.557 ± 0.062	19.367 ± 0.137	18.375 ± 0.079	18.476 ± 0.128
G_B	mag	18.200 ± 0.018	18.261 ± 0.049	19.101 ± 0.155	18.927 ± 0.193
G_C	mag	21.284 ± 0.065	21.107 ± 0.143	20.113 ± 0.073	20.212 ± 0.135
G_D	mag	19.225 ± 0.010	19.256 ± 0.027	19.597 ± 0.045	19.542 ± 0.073
i_S	mag	19.147 ± 0.062	18.972 ± 0.145	17.975 ± 0.070	18.074 ± 0.132
i_B	mag	17.362 ± 0.090	17.401 ± 0.034	17.870 ± 0.063	17.780 ± 0.102

Microlensing parallax constraint

Parallax effect in microlensing combined with the Gaia parallax

Mass - Distance constraint

$$M = \frac{\pi_l - \pi_s}{\kappa \pi_E^2}$$

Finite source effect constraint

θ_* derived from the color $g'-i'$ (Boyajian et al. 2014. Combining this with ρ_* we obtain the Einstein angle.

Mass - Distance constraint

$$M = \left(\frac{\theta_*}{\rho_*}\right)^2 \frac{1}{\kappa(\pi_l - \pi_s)}$$

Blend flux constraint

Conversion in V-band (Riello et al. 2021) Mass-luminosity relations for low mass star (Xia et al. 2008) Extinction map (Capitanio et al. 2017)

Mass - Distance constraint

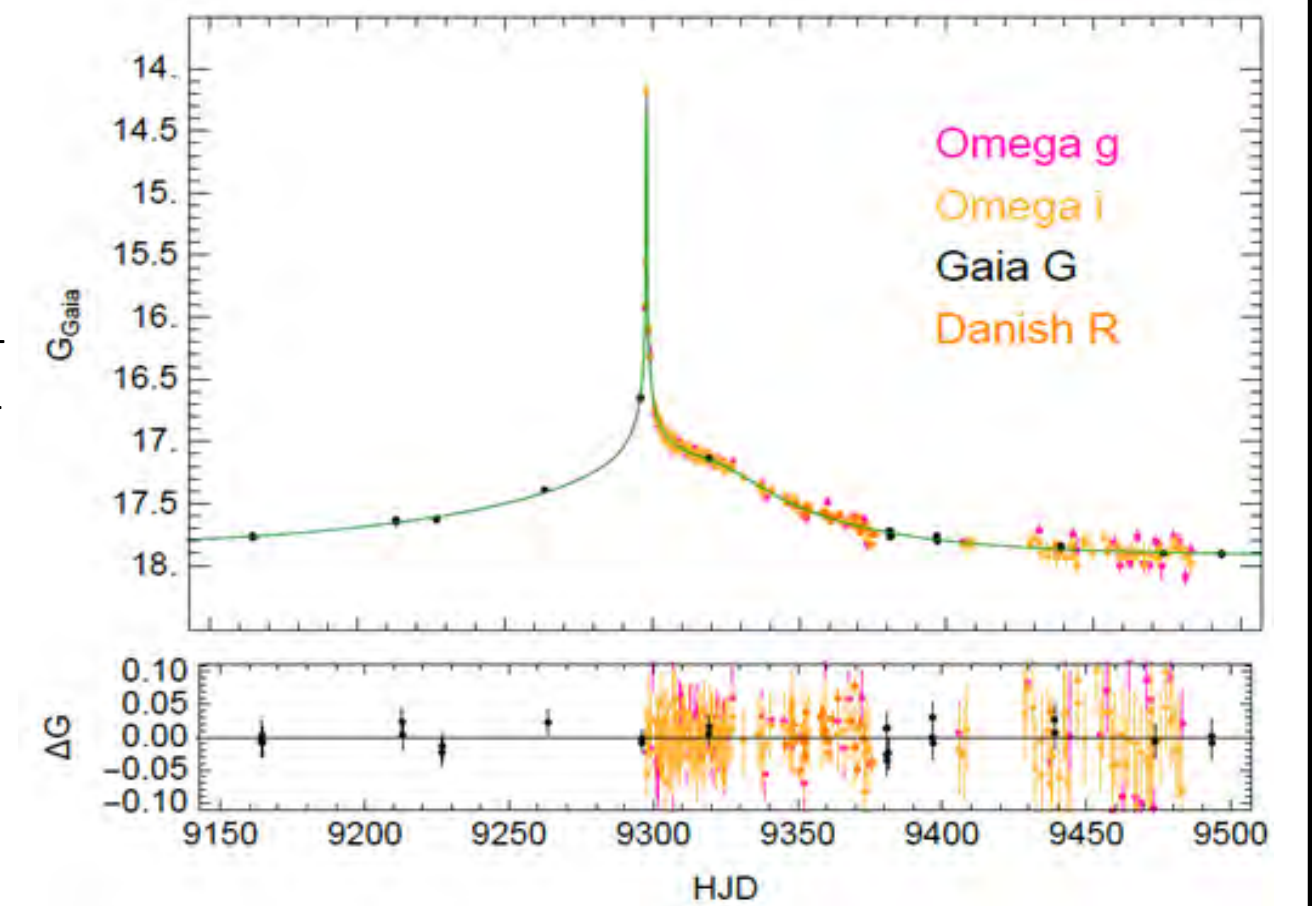
$$M_V(M) = m_V - 5 \log \frac{D_L}{10 \text{ pc}} - A_V(D_L)$$

Table 6. Physical parameters of lens and source for the best model C+

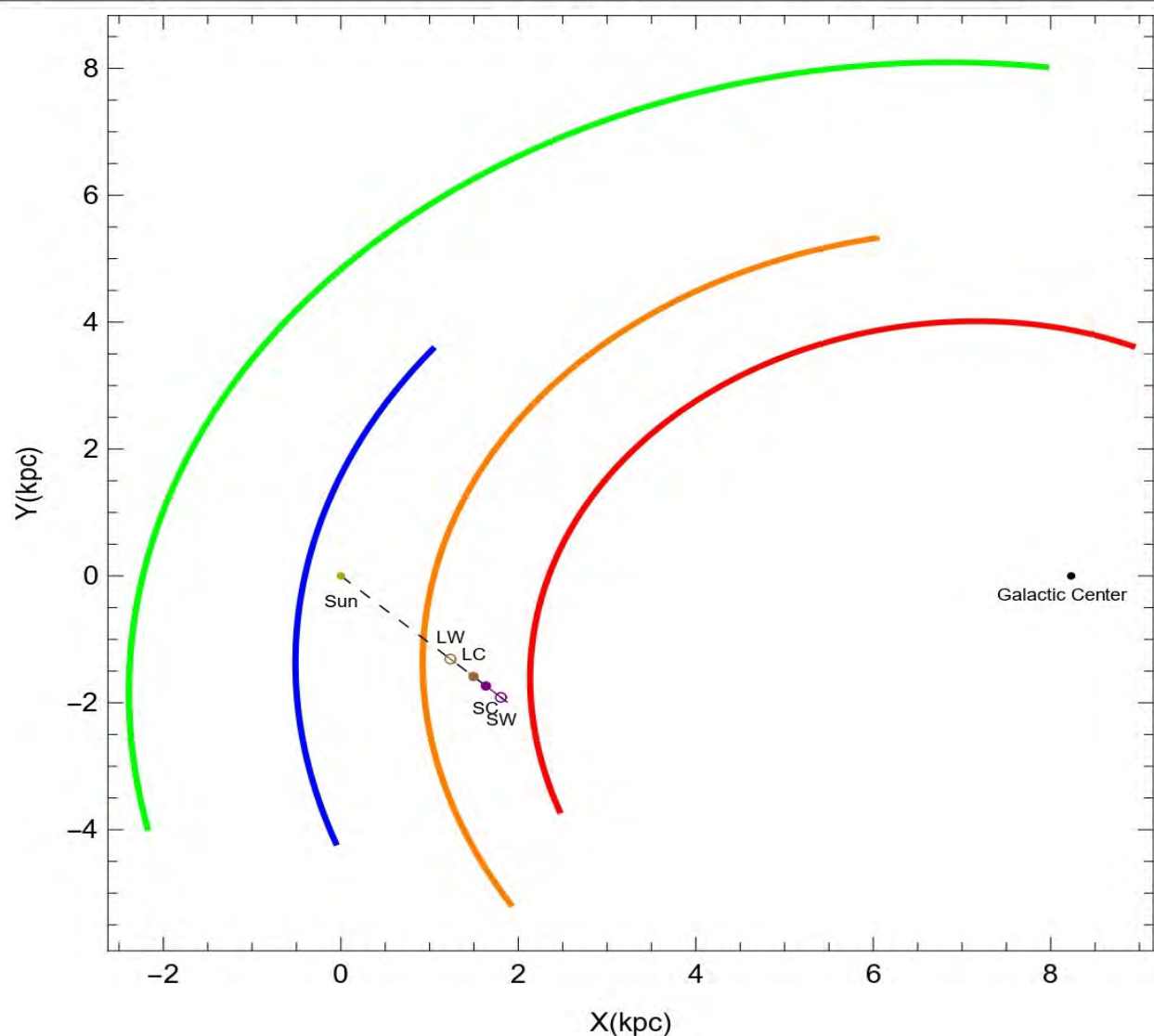
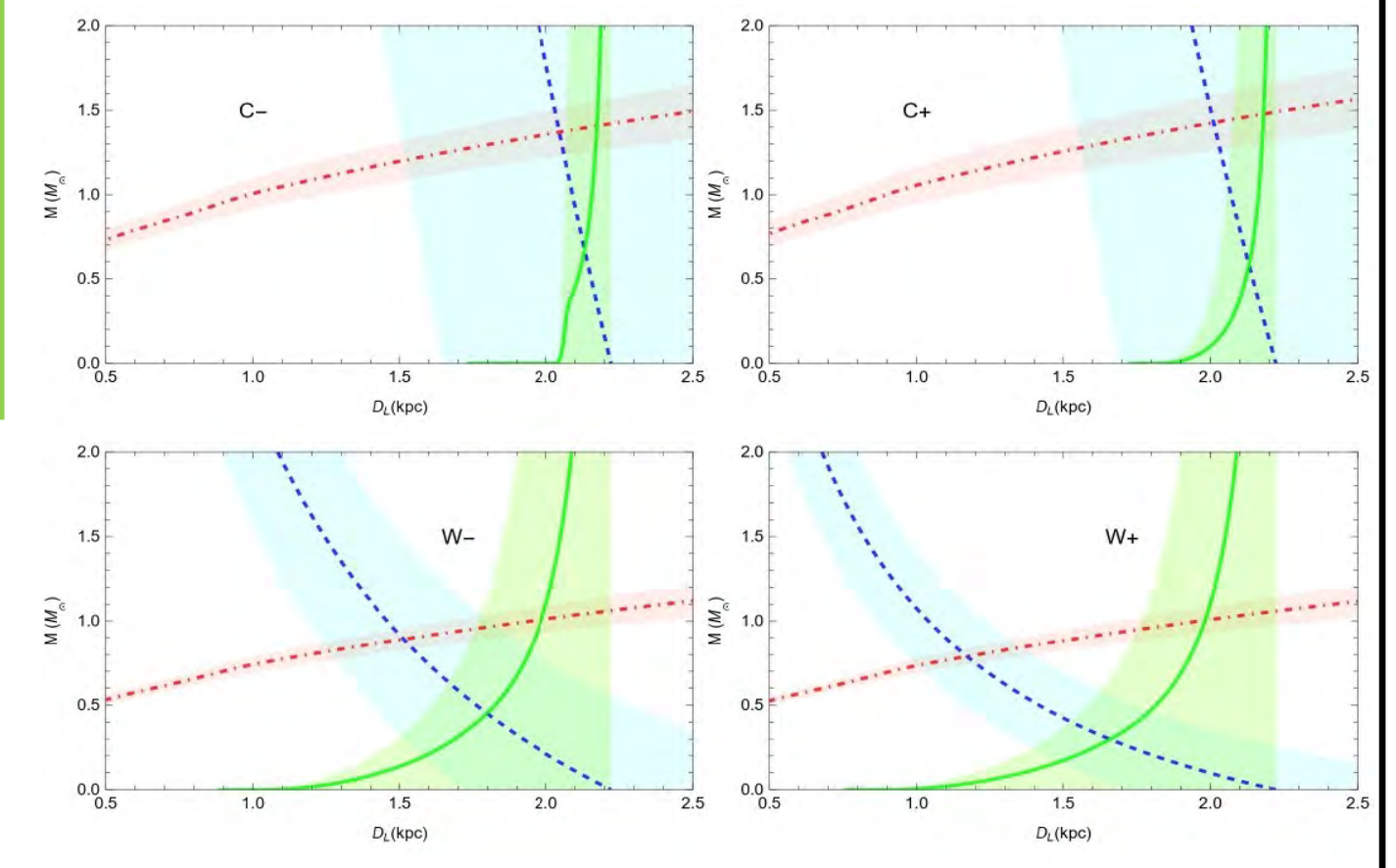
	Distance (kpc)	Mass (M_\odot)	g'	i'	G (Gaia)	Spectral class
Total lens	2.18 ± 0.07	1.48 ± 0.17	19.225 ± 0.010	17.362 ± 0.090	18.200 ± 0.018	-
Primary lens	2.18 ± 0.07	0.95 ± 0.12	20.023 ± 0.530	17.697 ± 0.530	18.016 ± 0.749	G star
Secondary lens	2.18 ± 0.07	0.53 ± 0.07	25.000 ± 0.514	20.601 ± 0.514	20.411 ± 0.727	K star
Source	2.38 ± 0.31	1.10 ± 0.18	21.284 ± 0.065	19.147 ± 0.062	19.557 ± 0.062	Subgiant F star

Table 7. Physical parameters of lens and source for the alternative model W-

	Distance (kpc)	Mass (M_\odot)	g'	i'	G (Gaia)	Spectral class
Total lens	1.79 ± 0.07	0.94 ± 0.09	19.542 ± 0.073	17.780 ± 0.102	18.927 ± 0.193	-
Primary lens	1.79 ± 0.07	0.78 ± 0.08	21.312 ± 0.653	18.306 ± 0.653	18.469 ± 0.924	K star
Secondary lens	1.79 ± 0.07	0.16 ± 0.02	29.551 ± 0.675	24.401 ± 0.675	24.575 ± 0.954	M star
Source	2.63 ± 0.10	0.96 ± 0.09	20.212 ± 0.135	18.074 ± 0.132	18.476 ± 0.128	G star



The three constraints appear as three colored bands whose width track the uncertainties at 1 sigma.



Bibliography

- [1] E. Bachelet, P. Rota, V. Bozza, Y. Tsapras et al. A close binary lens revealed by the microlensing event Gaia20bof. , In preparation
[2] P. Rota, V. Bozza, M. Hundertmark, E. Bachelet et al., Gaia21blx: complete resolution of a binary microlensing event in the Galactic disk , Submitted to Astronomy and Astrophysics

*Dipartimento di Fisica "E.R. Caianiello", Università degli studi di Salerno,
Via Giovanni Paolo II 132, I-84084 Fisciano (SA), Italy
Istituto Nazionale di Fisica Nucleare, Sezione di Napoli, Via Cintia, 80126
Napoli (NA), Italy
E-mail: prota@unisa.it